BER the international journal of bridge engineering management and research

A New Methodology for the Diagnosis and Monitoring of Bridges Under Slow Deformation Phenomena

Andrea Meoni[1,*]; Laura Ierimonti[1]; Elisabetta Farneti[1]; Matteo Castellani[1]; Filippo Filippucci[1]; Agnese Natali[2]; Simone Celati[2]; Fabrizio Scozzese[3]; Michele Morici[3]; Nicola Cavalagli[1]; Ilaria Venanzi[1]; Anil Kumar Agrawal[4]; Andrea Dall'Asta[3]; Walter Salvatore[2]; and Filippo Ubertini[1]

Submitted: 06 February 2024 **Accepted:** 05 April 2024 **Publication date:** 03 September 2024

Abstract: Roadway bridges can be subjected to several pathologies affecting their structural performance during operational conditions. Among others, slow deformation phenomena due to landslides often represent the primary cause of the onset of damage and collapse mechanisms. The timely identification of slow deformation phenomena on bridges and viaducts, as well as the evaluation of their extent and evolution over time, are therefore of crucial importance for preserving the safety conditions of road networks. In common practice, the preliminary analysis of slow deformation phenomena could be carried out over large geographical areas; hence, it can be used by managing institutions to set intervention priorities among the assets under their responsibility. In this regard, this paper proposes a new methodology for the diagnosis and monitoring of bridges under the effects of slow deformation phenomena based on the combined use of Synthetic Aperture Radar Interferometry (InSAR) techniques, visual inspections, geometric surveys, destructive and non-destructive testing methods, and numerical analyses. Specifically, InSAR is adopted to remotely identify bridges affected by slow deformation phenomena within large geographical areas/road networks. Then, visual inspections are carried out on the identified structures to investigate their defectiveness and the detected deformation phenomenon. Depending on the evaluated damage state, a bridge may be subjected to continuous InSAR monitoring, thus enabling the systematic analysis of the evolution of the deformation phenomenon and relevant anomalies over time or an accurate structural assessment via numerical analyses. In this last circumstance, information gathered from geometric surveys and field tests can be used for the fine-tuning of the numerical models of the structures. A practical application of the proposed methodology for the diagnosis and monitoring of a curved roadway bridge subjected to landslide phenomena is also presented in the paper for illustrative purposes. Overall, the results obtained in the case study provide a sound demonstration of the effectiveness of the proposed approach.

Author keywords: Structural health monitoring; SAR interferometry; operational modal analysis; numerical analysis; prestressed concrete bridges

Introduction

Bridges and viaducts are crucial infrastructural assets for transportation networks; in some cases, they also hold historical and strategic importance. To avoid significant losses both in terms of human lives and economic resources, it is essential to maintain their functionality, detect damage at early stages, and prevent collapses.[1–3] During their lifetime, bridges and viaducts can experience material deterioration, structural aging, direct damage due to natural hazards, such as earthquakes, strong wind, and so on, as well as damage due to slow deformation phenomena, such as landslides, subsidence, ground consolidation, foundation scouring, and prestress losses. In recent years, non-destructive techniques have been spreading out, underlying Structural Health Monitoring (SHM) methodologies. SHM involves the continuous acquisition and post-processing of data using contact or contactless sensing systems. This technology provides essential information about the structural integrity of constructions, reduces risks, and guides preventive maintenance interventions.[4–7] Recently, traditional SHM techniques have been paired with Synthetic Aperture Radar Interferometry (InSAR)-based methods. InSAR is a well-established technology that measures and monitors movements on the ground, exploiting SAR observations acquired by satellites orbiting at more than 500 km above the Earth's surface. This technique, which is particularly suitable for detecting and tracking slow deformations due to the dependence of the frequency of measurements on the satellite's revisit time over the area of interest, has recently been used for SHM of buildings and infrastructures.[8–14] The above-mentioned technique has significant benefits. Firstly, it allows for displacement information to be obtained on multiple points

*Corresponding Author: Andrea Meoni.
Email: andrea.meoni@unipg.it
[1]Department of Civil and Environmental Engineering, University of Perugia, Italy
[2]Department of Civil and Industrial Engineering, School of Engineering, University of Pisa, Italy
[3]School of Architecture and Design, University of Camerino, Italy
[4]Department of Civil and Environmental Engineering, The City College of the City University of New York, USA

of a single structure without having to access the site physically. Secondly, it can monitor vast regions or even entire bridge inventories at a relatively low cost. Additionally, high-resolution satellite acquisitions can provide millimeter-scale precision for displacement measurements along the Line of Sight (LOS), which connects the satellite radar antenna to the target on the Earth's surface. To cite a few examples of the most recent and prominent studies in the scientific literature dealing with InSAR-based bridge monitoring, in Farneti et al.,[15] a post-processing methodology has been developed that can use SAR observations from two different viewing geometries to derive a two-dimensional reconstruction of the bridge's movements over time and quantify the uncertainties of the estimated displacements. An approach to identify and classify bridges experiencing slow deformations in large assets, then assign them monitoring/assessment priority classes based on information from InSAR data, has been proposed in Nettis et al.[16]. The effectiveness of InSAR data for monitoring the structural response of diverse bridge components, such as access lanes, piers, spans, and bearing supports, thus allowing the identification of possible unexpected behavior, has been demonstrated in Tonelli et al.[17].

In this context, it is crucial to develop systematic methodologies to account for InSAR data, with the main objective of making informed decisions and scheduling interventions, minimizing risks, progressive damages, and costs in the management of bridge inventories. The exploitation of SAR technology can provide a fundamental contribution to pathologies understanding when properly combined with on-site structural monitoring and survey activities. In this paper, an integrated approach combining InSAR-based monitoring with the outcomes from visual inspections, geometric surveys, and additional non-destructive techniques is proposed for the diagnosis and monitoring of bridges and viaducts experiencing slow deformation phenomena, especially those caused by landslides. InSAR-based methods are utilized for remote detection of bridges affected by gradual deformation phenomena across road networks. On-site visual inspections are conducted on the identified bridges to evaluate their state of deterioration and the extent of detected deformation phenomena. Depending on the severity of their damage state, bridges may be subjected to continuous InSAR monitoring to track the progression of slow deformation processes or advanced numerical analysis to predict their remaining service life. The results of geometric surveys and additional non-destructive testing help to enrich the knowledge of bridges and refine numerical models for better estimation of their remaining life. The proposed methodology is applied to a real case study bridge characterized by critical structural defectiveness to provide a sound demonstration of the effectiveness of the approach. The rest of the paper is structured as follows. The proposed methodology is introduced together with the case study bridge and the performed experimental investigations. Then, the numerical models defined to replicate the mechanical response of the case study bridge are illustrated. Afterward, experimental and numerical results are presented. A closing section ends the paper, outlining comments and remarks.

Methodology Description

Fig. 1 illustrates the flowchart of the proposed methodology for the diagnosis and monitoring of bridges and viaducts under the effects of slow deformation phenomena due to landslides. The InSAR-based monitoring is adopted to remotely identify bridges affected by slow deformation phenomena within large geographical areas/road networks. SAR screening methods aim to identify assets exhibiting displacement histories characterized by clear trends indicating the accumulation of irreversible deformation over time, and therefore the progression toward a potential critical condition.

Once a bridge affected by permanent deformations is remotely identified, on-site visual inspections are carried out to assess and quantify the entity of the deformation phenomenon, hence its interaction with the asset. The defectiveness of the selected structure is also evaluated and compared with the results from past inspection activities when available. This last operation can provide meaningful indications of the evolution over time of the defects detected on the asset. Based on the outcomes from visual inspections, the methodology proposes two different monitoring strategies for the asset under investigation. In the first scenario, a data-driven SHM approach is adopted. Specifically, a bridge can be subjected to continuous InSAR monitoring when the outcomes from visual inspections do not highlight critical structural conditions. In this circumstance, therefore, the remote monitoring of the asset is primarily aimed at

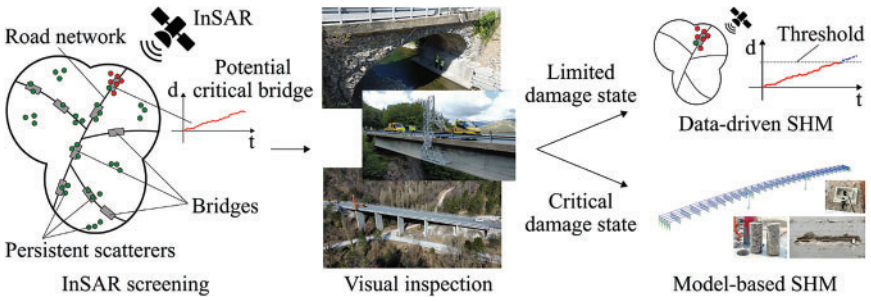

Figure 1. Conceptual flowchart of the proposed methodology for the diagnosis and monitoring of bridges under the effects of slow deformation phenomena

detecting potential anomalies in the evolution of the slow deformation phenomenon at an early stage. Alarm thresholds related to the trends of the displacements monitored via InSAR can be set based on engineering judgment, which may consider the typology of the bridge, its static scheme, and the features of the landslide, to name a few. When one or more thresholds are triggered, the authority responsible for the asset under continuous InSAR monitoring is promptly informed, and further inspections may be carried out on the bridge to assess its actual structural condition. Advanced processing of InSAR data can also be carried out to obtain information on the structural performance of the selected bridge. As an example, the evolution of the deformed configuration of the asset can be reconstructed to investigate potential alterations induced over time by the landslide-structure interaction. In the second scenario, namely when visual inspections point out critical structural conditions for the asset remotely identified via InSAR monitoring (e.g., due to the high defectiveness or the initiation/progression of damage mechanisms), a model-based SHM approach is considered. A numerical model of the asset under investigation is constructed and hence used to perform collapse simulations and estimate the residual life of the structure. The outputs from numerical analyses are used to integrate/validate those obtained from the processing of InSAR data and vice versa, thus achieving a comprehensive evaluation of the structural performance of the asset. In this scenario, extensive geometric surveys are carried out to aid the comprehension of the bridge-landslide interaction. Furthermore, field tests, including additional non-destructive techniques, can be performed on the asset to evaluate materials' mechanical properties, as well as potential modifications in the static and dynamic response of the structure with respect to its design configuration. The outcomes from field tests can also contribute significantly to the fine-tuning of the numerical model used to perform structural assessments.

Application Case Study

This section presents the case study bridge and the experimental investigations carried out to characterize its actual defectiveness and structural response.

Bridge description

The case study bridge [see Figs. 2a and 2b] has a planimetric development with a curved shape, with a total length of 66 m, measured along the supports. It has a static scheme of continuous beams on four supports (the right and left abutments plus two piers), with a central span of 36 m and two side spans of 15 m each. The deck of the bridge has a width of 7.50 m, of which 6.50 m is used for the carriageway and 0.50 m on each side for the safety barriers. The superstructure consists of a post-tensioned concrete slab with a rectangular cross-section and dimensions of 4.50 m × 1.10 m, from which two symmetrical cantilevers, each projecting 1.5 m, extend laterally [Fig. 2c]. The slope of the carriageway is constant and equal to 4% and 6% along the transversal and longitudinal directions, respectively. The piers are made of two overlapping elements; the lower element is made of ordinary Reinforced Concrete (RC), while the upper one is a slender rectangle-shaped RC element, which is equipped with a cylindrical hinge bearing support at the base and top and thus has a pendulum function; its rectangular cross-section has dimensions of 4.50 m × 0.90 m, measured between the hinges. The lower portion of the right pier is formed by a parallelepiped-shaped RC structure with a plan view section of 2.00 m × 4.50 m and a height of 4 m, which is made integral with the foundation plinth. The lower portion of the left pier is made of a first parallelepiped-shaped RC structure with a rectangular section of 2.00 m × 6.95 m and a height of 16 m, with an enlargement of 2.50 m in width and a height of about 2.00 m [see Fig. 2d]. Unlike the right pier, the left pier has a direct foundation, given the presence of the underlying rocky layer. The left abutment, connected to the superstructure by movable bearing supports, is made of RC and stands on a direct foundation. The height of the front wall, measured from the top of the foundation to the plane of the bearing supports, is 6.64 m, while the height of the foundation plinth is 1.50 m. The right abutment is the site of a fixed bearing support and is realized through an RC structure of variable height. In the downhill section, the front wall, measured from the top of the foundation to the support plane of the bearing supports, has a height of 3.25 m, while in the uphill section, it has a height of 1.50 m. The bridge is subject to a mountain landslide, inducing the deck to move towards the right abutment. As a result, the structure is characterized by critical defectiveness, as described in the following sections.

InSAR-based monitoring

To derive the temporal evolution of the displacements affecting the case study bridge, two stacks of SAR images acquired over the area of interest by the Italian satellite constellation COSMO-SkyMed were analyzed. The first dataset, acquired in ascending geometry (i.e., when the satellite navigates approximately from the South to North poles), was composed of 51 images covering the period between January 2018 and December 2021; the second set of images, acquired in descending pass (i.e., when the satellite travels from the North to South poles) consisted of 78 acquisitions recorded in the period between January 2018 and January 2022. The direction cosines of the ascending and descending LOS over the area of interest are summarized in Table 1. Processing the two image datasets through the Persistent Scatterer Pair (PSP) technique,[18] it was possible to extrapolate the displacement information for a set of sparse points, called Persistent Scatterers (PSs), located on the monitored structure and the ground in its proximity and corresponding to radiometrically stable targets within the monitoring period. The position of the detected PSs had a metric precision in the three-dimensional space. In contrast, the associated displacement measurements had a millimeter-scale precision along the LOS direction, which connects the satellite radar antenna with the target on the ground.

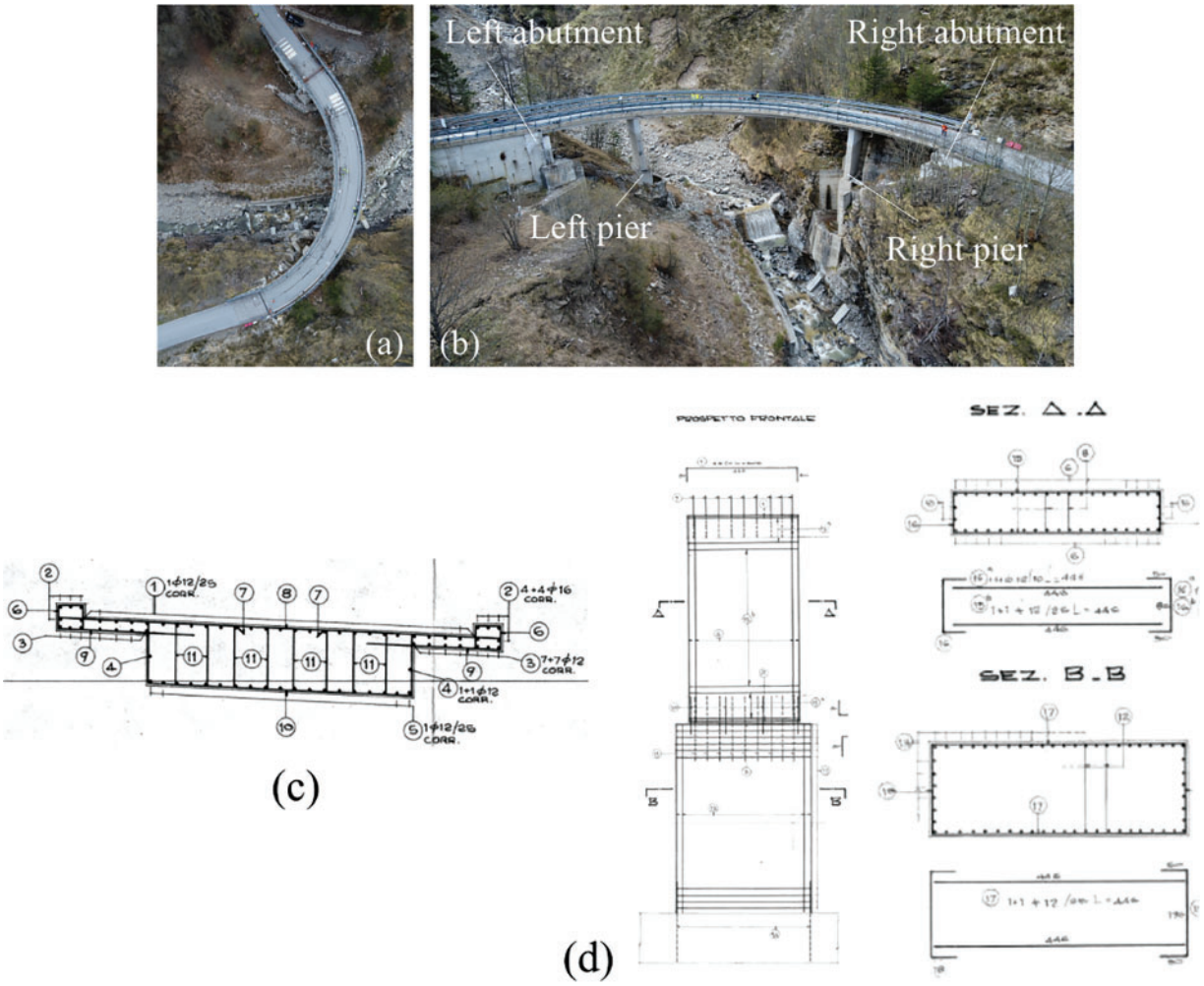

Figure 2. The case study bridge: (a) aerial view; (b) lateral view; (c) cross-section of the deck retrieved from the original technical drawings; (d) construction details of the left pier retrieved from the original technical drawings

Table 1. Direction cosines of the ascending and descending LOS of COSMO-SkyMed satellites over the studied area

	East	North	Vertical
Ascending geometry	−0.441646	−0.082075	0.893427
Descending geometry	0.548311	−0.1120473	0.828734

Geometric surveys

A photogrammetric survey was conducted on the case study bridge to detect its geometry and structural configuration. Fig. 3 shows the conceptual flowchart describing the main steps of the geometric survey conducted through Unmanned Aerial Vehicle (UAV) photogrammetry. A drone model DJI Mini 2, with a 1/2.3″ CMOS sensor with 12 MP, was employed to scan the bridge by carrying out a total of nine flight missions. Six flights were carried out with the camera tilted zenithally by 60° and 45° to properly scan the deck of the bridge. Furthermore, three detailed flights, with a camera angle of 0° and 30°, were carried out to scan both piers. All the flight routes were carried out manually due to interfering vegetation. The percentage of overlap between the individual frames was equal to 80%. The acquired set of images was processed with a Structure from Motion software, named Metashape from Agisoft, to extract the point cloud of the sampled surfaces. Once obtained the point cloud of the bridge, hence converted to a textured 3D model, orthophotos of the piers were extracted with a Ground Sample Distance value of 7.09 mm/px. These pictures were further analyzed to determine the actual inclination of the piers with respect to the original configuration of their vertical axis.

Ambient vibration tests and modal identification

The dynamic behavior of the case study bridge was investigated by performing Ambient Vibration Tests (AVTs) on April 27th, 2022. Acceleration measurements were carried out according to the setups illustrated in Fig. 4 by using high-sensitivity (10 V/g) uniaxial seismic accelerometers, model PCB393B12, installed on stabilization steel supports positioned on the concrete curbs of the bridge deck.

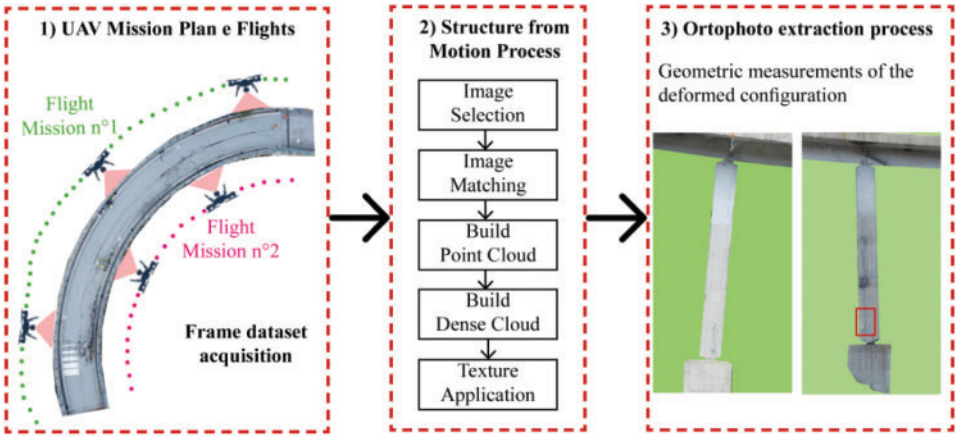

Figure 3. Conceptual flowchart describing the main steps of the geometric survey conducted on the case study bridge through UAV photogrammetry

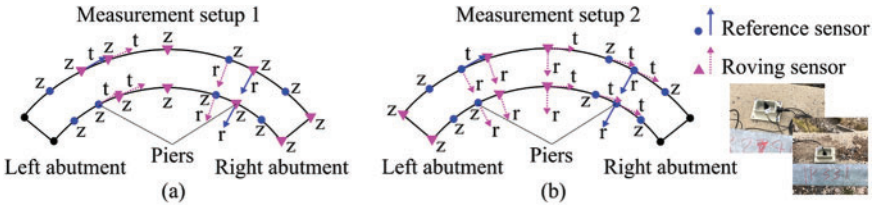

Figure 4. Measurements setups used to perform ambient vibration tests on the case study bridge

A data acquisition system (DAQ), model NI cDAQ-9188, embedding four NI 9234 modules and three NI 9230 modules, was used to acquire vibration measurements with a sampling frequency of 1706 Hz. Each measurement record lasted thirty minutes, a time window quite larger than 2000 times the fundamental period of the bridge, which usually ensures an accurate estimation of the modal parameters.

The dynamic identification of the structure was carried out by using MOVA, a software for Operational Modal Analysis (OMA) recently developed by the University of Perugia.[19] The set of accelerations recorded for each measurement setup was detrended and resampled at 40 Hz, hence processed for modal feature extraction (natural frequencies, damping ratios, and mode shapes) with the Enhanced Frequency Domain Decomposition (EFDD) method. The mode shapes of the case study bridge were determined using the least squares approach to merge the shapes identified from the analysis of each measurement setup.[20]

Dynamic traveling load tests

A series of dynamic tests under traveling loads were carried out on the case study bridge to collect information about its response under service loads. The tests exploited the input provided by the passage of a vehicle of known mass and speed, while the response measurements were obtained from longitudinal strain sensors placed at the deck extrados of the bridge. The sensor setup was designed by taking advantage of the symmetry of the system; three measurement points (S1, S2, and S3) were identified at the extrados of the deck in correspondence with the right pier and the midspan sections of spans 2 and 3, as shown in Fig. 5a. The sensor typology used to measure deformations consists of a strain gauge bar installed on the bridge deck, as shown in Fig. 5b, internally equipped with four strain gauges connected according to a complete Wheatstone bridge circuit. The vehicle used to excite the bridge was a van weighing approximately 2000 kg. Given the conditions of the bridge, it was decided not to opt for heavier vehicles. The vehicle traveled at a constant speed of 30 km/h from Span 1 to Span 3 and vice versa; the travel was repeated twice [see Fig. 5c].

Numerical Models of the Case Study Bridge

This section presents the numerical models used to evaluate the actual structural response of the case study bridge and to provide a preliminary estimate of its residual life.

Simulation of the design structural configuration

A first numerical model was defined to simulate the design structural configuration of the case study bridge. The Finite Element (FE) model, shown in Fig. 6a, was built in SAP2000[21] by using eight-node solid elements to discretize the geometry retrieved from the available design reports. Cylindrical hinge restraints were applied on the right-hand side of the model's deck end to simulate the connection with the abutment. In contrast, two multidirectional and two one-directional restraints were placed on the outer and middle ends of the left side of the model, respectively, to replicate the connection with the other deck abutment. To reproduce the pendulum behavior of the piers, cylindrical hinge restraints were applied at the basement of both model's piers, while

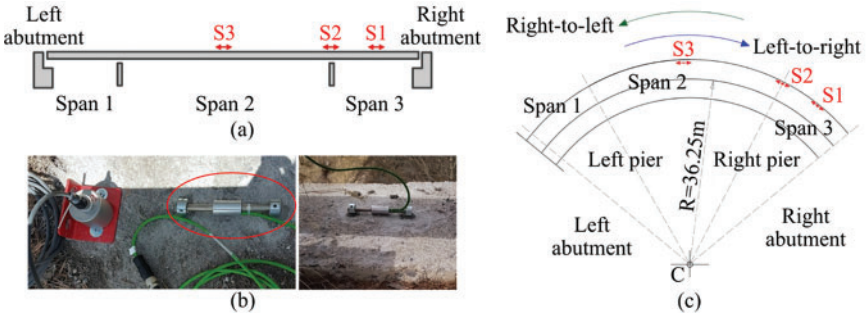

Figure 5. Dynamic traveling load tests: (a) measurements setup; (b) pictures of strain gauge bars installed on the bridge deck; (c) schematic representation of the vehicle travel directions

Figure 6. Numerical model of the case study bridge: (a) global view; (b) details of piers modeling

Table 2. Design mechanical properties assigned to the numerical model of the case study bridge: f_{ck} is the characteristic compressive strength of concrete, E is its elastic modulus, v indicates the Poisson's coefficient, and ρ is the density

Structural element	f_{ck} [MPa]	E [MPa]	v	ρ [kg/m^3]
Deck	32	33346	0.2	2499
Piers	28	32308	0.2	2499

triangular elements with vertex nodes joined to the deck nodes were modeled at their top section [see Fig. 6b]. This modeling strategy allows relative rotations between the deck and the pillars of the model, yet not relative translations. Table 2 collects the design mechanical properties, taken from the original technical reports, used to specialize the linear elastic response of the numerical model.

Simulation of the actual structural configuration

A second numerical model was defined in SAP2000 to reproduce the actual structural configuration of the case study bridge. The model's geometry was defined by using the outcomes from the UAV photogrammetry campaign, while its mechanical properties were initially set equal to those of the model described in the previous section. The detachment of the bearing supports, observed at the left abutment of the bridge by performing visual inspections and UAV photogrammetry, was simulated by positioning the bearing supports of the model towards the inside of the deck curvature. At the right abutment, the deck of the model was constrained along the three main directions to reproduce the actual deck-abutment interaction. To represent the partial detachment observed at the base and top of the left pier due to its transverse rotation, restraints were removed at the detached part of the base of the left pier, hence triangular solid elements, connecting the top of the pier with the model's deck, were removed at the detached part of the top of the left pier. No modifications were made to the position of the restraint systems on the right-hand pillar of the numerical model. Lastly, all the restraints of the numerical model were replaced with link elements connecting the model to the ground. The stiffness of these connections was appropriately calibrated to replicate the dynamic behavior of the structure observed from field measurements as closely as possible. In this regard, the elastic moduli of the model were also involved in the fine-tuning. The calibration procedure consisted of estimating the modal properties of the numerical model representing the actual structural configuration of the bridge through numerical simulations and comparing them with the experimental modal features. The analysis focused on the first three identified modes of vibration. Experimental and numerical vibration frequencies were tested in terms of relative variations, while the Modal Assurance Criterion (MAC) was adopted to evaluate the consistency between experimental and numerical mode shapes.[22] A comparison in terms of vibration frequencies was also carried out between the numerical model representing the design structural configuration of the bridge and that representing the actual structural configuration. This latter analysis made it possible to assess the changes that occurred in the dynamic response of the structure due to the landslide-structure interaction compared to the initial design.

Simulation of the collapse mechanisms

Numerical simulations were carried out to assess the structural performance of the case study bridge under the evolution of the landslide phenomenon. Considering the direction of the mountain landslide [see Fig. 7a], known from past monitoring activities, increasing displacements simulating the movement of the ground were applied to the left pier and abutment of the numerical model representing the actual structural configuration of the bridge to investigate the potential collapse mechanisms. The growth rate of the landslide was assumed to be constant over time. A first set of increasing displacements, whose maximum entity was equal to 300 mm, was applied to the left pier of the model. This is because the left abutment of the bridge can

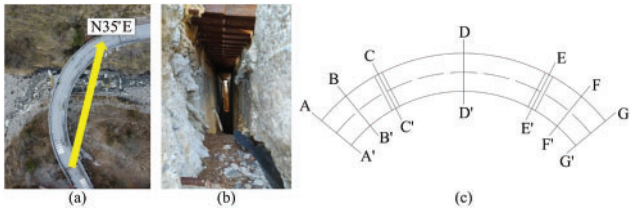

Figure 7. Numerical simulation of the landslide evolution: (a) landslide direction; (b) gap between the back wall of the left abutment and the deck of the case study bridge; (c) bridge sections verified under unsymmetrical bending

move towards the deck for about 300 mm before making contact with this structural part; this distance represents the gap between the back wall of the left abutment and the deck, as shown in Fig. 7b. A second set of increasing displacements was then applied to the left abutment of the numerical model, thus simulating the evolution of the landslide with the left abutment in contact with the deck. In this circumstance, the internal stress state of the model's deck increased at every increment in the applied displacements. The structural assessment of the bridge was carried out by considering the fundamental combination of dead and live loads at the Ultimate Limit States (ULS) established by Eurocode 0,[23] hence by assuming a confidence factor equal to 1.35 for materials' strengths according to Eurocode 8[24] (i.e., a limited knowledge level was considered for the structure under investigation to analyze the worst-case scenario). Unsymmetrical bending verifications of the deck at ULS were carried out at the sections illustrated in Fig. 7c. Thus, the maximum admissible displacement of the left abutment, corresponding to the crisis of the first section of the bridge among those tested, was determined.

Results

This section outlines the results obtained from the experimental investigations carried out on the case study bridge and the outcomes from the numerical simulations performed.

InSAR data analysis

The PSP analysis performed on the two image datasets allowed the detection of a certain number of measurement points on the deck of the case study bridge and the neighboring ground. The obtained ascending and descending velocity maps are shown in Fig. 8. In the plots, the PSs are color-coded based on their mean velocity in the monitored period. Focusing on the time histories of the PSs identified on the deck. It is highlighted that the portion of the bridge on the side of the left abutment is affected by an evident accumulation of irreversible deformations in the four-year time window covered by the satellite acquisitions, for both ascending and descending analyses. In particular, in ascending geometry, the PSs exhibit time series with a negative trend, while the PSs identified in descending geometry are characterized by a positive trend. Since the provided measurements are the projections of the real displacement vectors along the LOS in the considered viewing geometry, the opposite sign of the LOS displacement trends in ascending and descending geometries conceivably indicates that the actual movement of the deck has a prevailing horizontal component with respect to the vertical one. The permanent deformations detected through InSAR monitoring on the structure can therefore be related to the effects of the slow progression of the landslide in the period 2018–2021. In addition, the post-processing of SAR data (described in detail in Farneti et al.[25]) highlighted a rate of about 43.8 mm/year, characterizing the deformation phenomenon affecting the left abutment of the bridge.

Given the insights from the InSAR data analysis performed, the case study bridge was classified as a potentially critical asset affected by slow deformation phenomena. According to the methodology proposed in this work, on-site visual inspections were carried out on the structure to evaluate its health state and the entity of the interfering landslide.

Defectiveness of the bridge

On-site visual inspections were carried out on the case study bridge to assess its structural defectiveness once the outcomes from InSAR screening highlighted that the bridge was affected by permanent deformations due to slow deformation phenomena. As a result of the bridge-landslide interaction, the deck of the bridge was found stuck in the right abutment following the failure of the fixed bearing supports, as shown in Fig. 9a. Furthermore, the sliding supports at the left abutment were damaged and detached from the deck of the bridge [Fig. 9b]. The left pier was tilted in both its vertical and transversal plane because of the sliding of its foundation. These rotations caused a partial detachment between the deck and the upper part of the pier. A partial detachment was also noted at the interface between the pier and its foundation, as depicted in Fig. 9c. The right pier was also rotated in both its vertical and transversal plane due to the sliding of the deck towards the right abutment. Based on the described defectiveness, the actual structural configuration of the bridge is far from the design configuration, and therefore classifiable as critical. In compliance with the proposed methodology, the model-based SHM approach was chosen to assess the structural performance of the asset.

Geometrical surveys

The UAV photogrammetry campaign carried out on the case study bridge resulted in a point cloud consisting of about 2.6×10^7 points, created from a dataset of 167 images. Fig. 10a shows the textured 3D model of the bridge obtained from the further processing of the point cloud. In contrast, Fig. 10b details the actual structural configuration of the piers of the bridge. The processing of the orthophotos of the left pier highlighted an inclination of its vertical axis of about 3.6° with respect to its original configuration, with a maximum horizontal displacement at the top of the pier

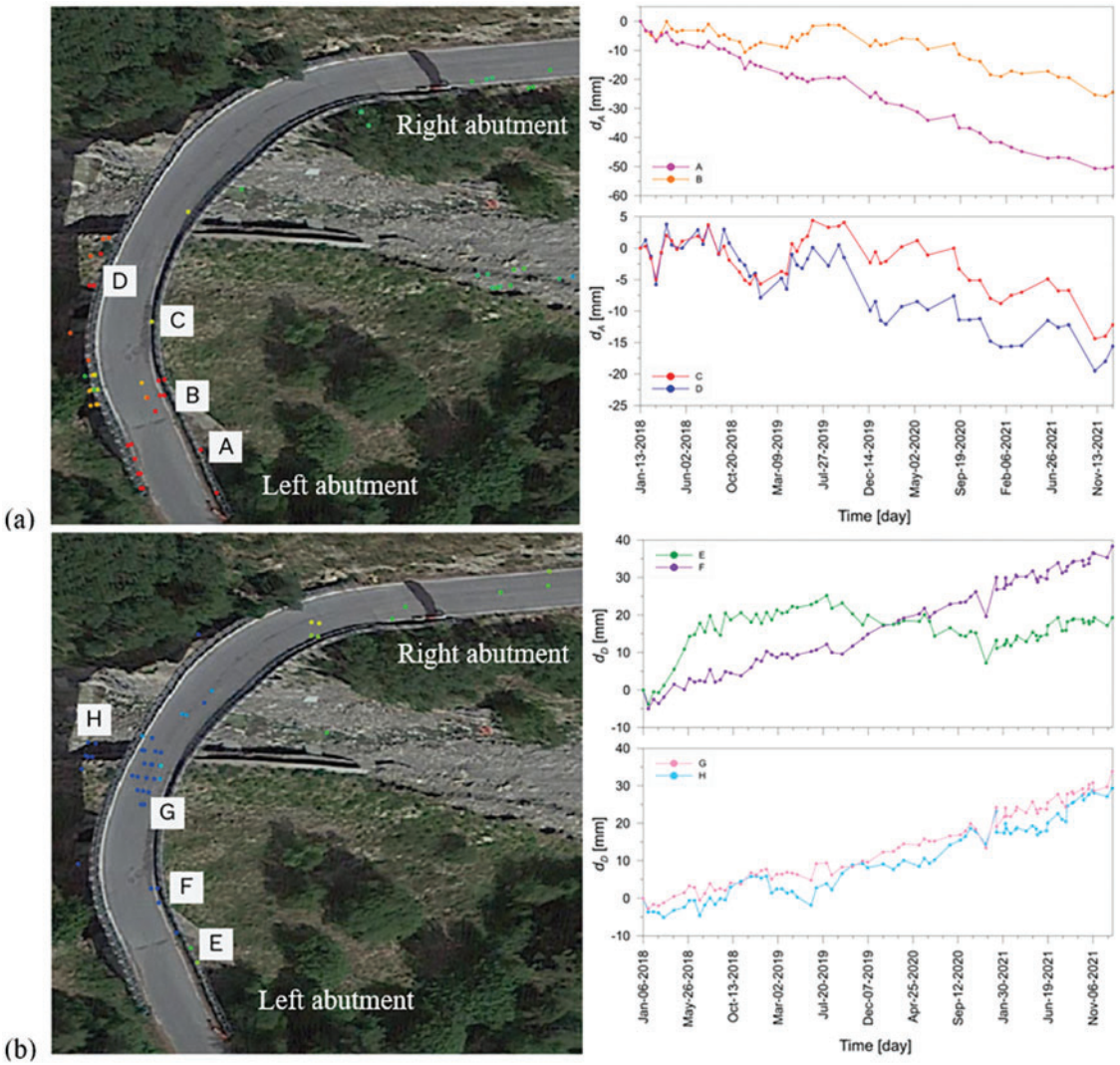

Figure 8. PSs detected in (a) ascending and (b) descending geometry on the bridge deck; the time series of four PSs are shown in both geometries, two identified close to the left abutment and two on a portion of the deck above the left pier (positive values indicate movements towards the satellite's antenna)

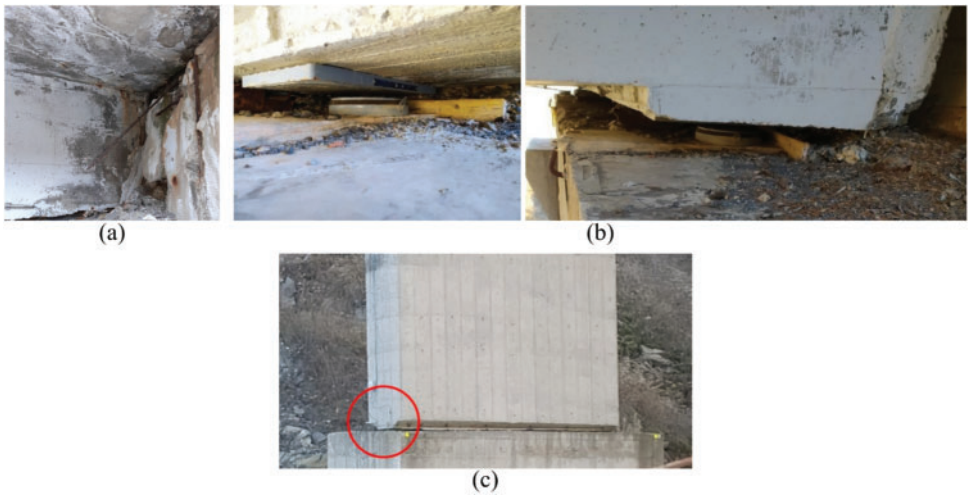

Figure 9. Defectiveness of the case study bridge: (a) detail of the bridge deck-right abutment interlock; (b) pictures of the detachment of the bearing supports at the left abutment; (c) partial detachment at the interface between the left pier and its foundation

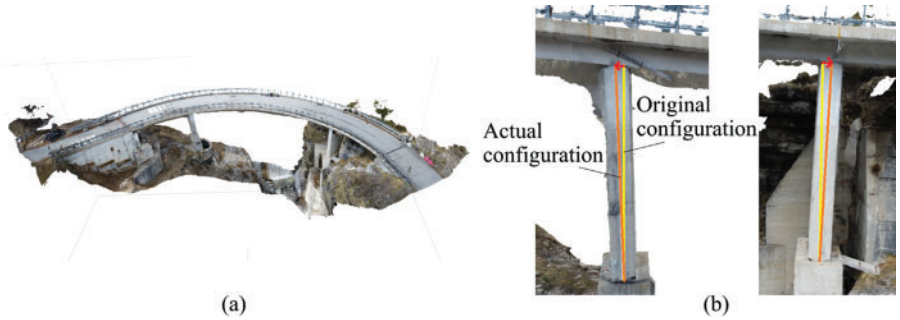

Figure 10. Results from the UAV photogrammetry campaign: (a) textured 3D model of the case study bridge; (b) actual inclination of the piers with respect to their original vertical axis

of 37 cm towards the left abutment. Similarly, the vertical axis of the right pier was tilted by about 2.2° with respect to its original configuration, with a maximum horizontal displacement at the top of the pier of 32 cm towards the right abutment.

Experimental and numerical characterization of the dynamic behavior of the bridge

Natural frequencies and mode shapes characterizing the dynamic behavior of the case study bridge are depicted in Fig. 11. The identified mode shapes point out unexpected torsional movements of the bridge deck at the left abutment and pier. These anomalous movements of the structure indicate the occurrence of modifications at the bearing supports with respect to the initial design, whose origin can be attributed to the effects of the landslide of the mountainside. Table 3 reports the relative variations between the natural frequencies of the bridge and those obtained from the numerical simulation of its design structural configuration and actual structural configuration. It is interesting to note that the numerical model representing the design structural configuration did not simulate the second mode of vibration of the structure. This is because the second mode of vibration characterizes the dynamic response of the bridge following the modifications induced by the landslide to the structural configuration of the left pier. On the other hand, once properly calibrated, the numerical model simulating the actual structural response of the structure was able to replicate the natural frequencies corresponding to the first three modes of vibration observed experimentally. In this last model, to improve the match with the natural frequencies experimentally determined, an elastic modulus equal to 39000 MPa and 37000 MPa was set to specialize the mechanical response of the concrete of the deck and piers, respectively.

Table 3. Relative variations between the natural frequencies determined experimentally and those obtained from the numerical models representing the design structural configuration and the actual configuration of the case study bridge

Mode of vibration	f_{exp} [Hz]	$f_{initial\ model}$ [Hz]	Variation [%]	$f_{calibrated\ model}$ [Hz]	Variation [%]
1	2.3732	2.2989	+3.13	2.3246	+2.05
2	5.8600	–	–	5.8674	−0.13
3	6.5049	6.4269	+1.20	6.5159	0.17

Table 4 reports the values of the MAC computed by comparing the experimental mode shapes of the first three vibration modes with those retrieved from the calibrated numerical model. The values reported in the diagonal of the MAC matrix indicate that the model consistently replicated

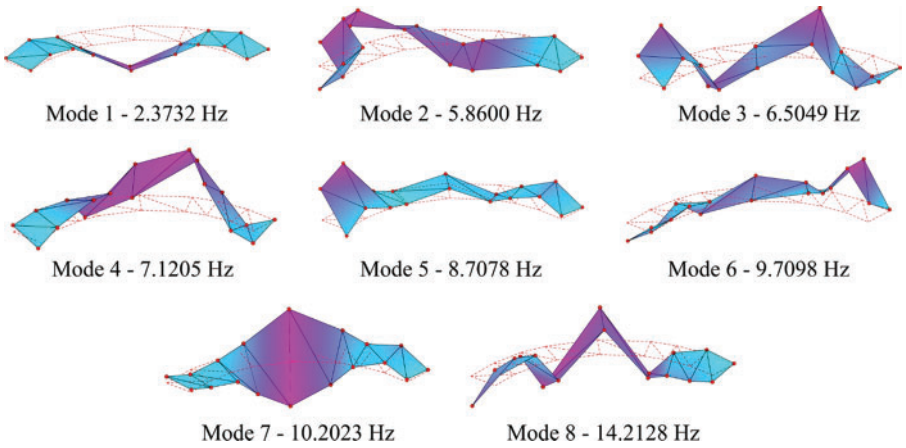

Figure 11. Natural frequencies and mode shapes of the case study bridge

Table 4. MAC matrix expressing the consistency between experimental and numerical mode shapes

Experimental mode of vibration	Numerical mode of vibration		
	1	2	3
1	0.98	1.4E−3	8.2E−4
2	2.4E−6	0.84	0.12
3	1.1E−4	3.3E−4	0.46

Figure 12. Mode shapes and natural frequencies obtained from the numerical model simulating the actual structural response of the bridge

the shapes of both the first and second modes of vibration of the bridge. Although the model effectively reproduced the frequency of the third mode of vibration, some discrepancies between the experimental and numerical shapes of this mode remained at the end of the calibration procedure, as indicated by the low value of MAC obtained from their comparison. The modal features obtained from the numerical model simulating the actual structural configuration of the bridge are shown in Fig. 12.

Results from dynamic traveling load tests

Results from dynamic traveling load tests are presented in terms of deformation time histories recorded in the traveling time interval. The charts in Fig. 13 compare the responses related to the three sensors S1, S2, and S3 (red Span 3, blue Span 2, orange right pier, respectively). The response of the bridge to the passage of the vehicle from Span 3 to Span 1 is shown in Fig. 13a, and the one from Span 1 to Span 3 in Fig. 13b. The time interval reported in the figures is equal to 12 s, of which the first 0.9 s represents the response of the bridge before the vehicle enters the bridge (i.e., the 0.9 s before the positioning of the front axle of the vehicle on the abutment expansion joint), the next approximately 9.0 s characterize the bridge response when the vehicle is actually traveling on it; the tails of the signals (about 2.0 s long) represent free vibration response of the bridge after the passage of the vehicle. Focusing on the chart in Fig. 13a, it can be seen how the sensor S1 (Span 3—red curve) exhibits its maximum negative deflection after 2.0 s, i.e., in the time instant at which the vehicle is in the middle of Span 3; the maximum positive deflection of Span 3 is observed when the vehicle crosses the middle section of Span 2, i.e., approximately around 5.5 s; finally, when the vehicle approaches the middle section of Span 1, it is again observed a negative deflection of Span 3 (around 8.5 s) but of notably reduced magnitude. The time history of strains from sensor S3 (Span 2—blue curve) attains its maximum (negative) in correspondence of 5.5 s (i.e., when the vehicle crosses the section at which sensor S3 was placed); two symmetric positive deflection peaks can be observed at 2.0 and 8.5 s, corresponding to the passage of the vehicle on the midspan of Span 3 and Span 1, respectively. The interpretation of the time history of strains recorded from sensor S2 (right pier—orange curve), unlike the previous two, is less straightforward, and it is the result of the boundary conditions modification produced by the landslide of the mountainside (e.g., bearing supports with imperfect contact; partial support of the piers due to detachment at the bottom interface with foundation structure). Similar comments can be made for the results shown in Fig. 13b, related to the vehicle motion from the left to the right abutment.

The dynamic response of the bridge subjected to vehicle passages was numerically simulated by exploiting a simplified FE model in which the bridge deck and piers were represented by elastic shell elements, thus significantly reducing the computational cost of the analyses compared to the solid-element models previously described. However, the geometry of the simplified model was based on the performed geometric surveys, ensuring that it reflected the actual structural configuration of the case study bridge, as well as its response, was properly refined by considering the outcomes from modal identification. A comprehensive description of the simplified FE model and the adopted calibration procedure can be found in Celati et al.[26]. It is worth noting that, despite the model's materials being elastic, a nonlinear dynamic time-history analysis was performed to catch the nonlinearity of the boundary conditions (i.e., gap elements were used to simulate the imperfect contacts between structural parts). In Fig. 14, a comparison is provided between the deformation time histories recorded by the sensors installed on the bridge deck and those numerically simulated through the simplified FE model. In the plots, the abscissa has been normalized to eliminate the influence of the imperfect match between numerical and experimental traveling times. Despite the complexity of the case study and related boundary conditions, the agreement between numerical and experimental results appears satisfactory, thus testifying to a quite high degree of reliability of the model. Furthermore, this is also witness to the fact that the bridge deck, under the investigated dynamic loads, remains in the linear elastic field of behavior.

Overall, the results from the dynamic traveling load tests confirmed the presence of structural critical issues highlighted by both visual inspections and other experimental campaigns (e.g., OMA). Moreover, the present application represents a preliminary test of the capability of damage detection strategies based on strain measures under moving vehicles, which revealed that it is suitable to explore potential anomalous responses of bridges due to multiple causes (landslide in this specific case).

Prediction of the residual life of the structure

Fig. 15 shows the deformed configuration of the numerical model of the case study bridge obtained by simulating the evolution of the mountain landslide over time. The first set of displacements applied to the left pier of the numerical model induced a translation of 300 mm of the base of the left pier

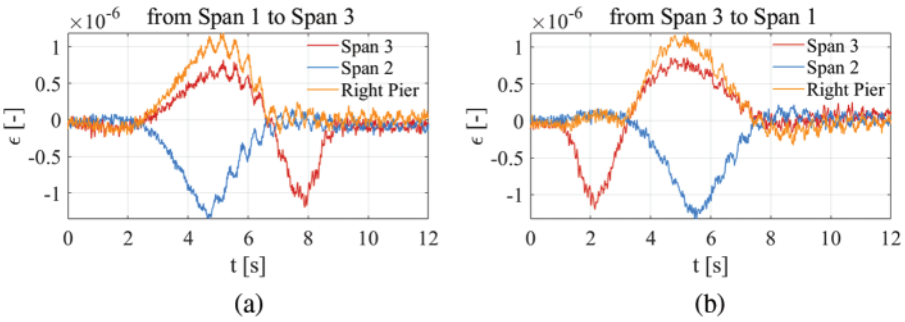

Figure 13. Comparison of the deformation time histories recorded by the sensors (placed at the midspan extrados of Spans 2 and 3 and at the top of the right pier) during the passage of the vehicle: (a) from Span 3 to Span 1; (b) from Span 1 to Span 3

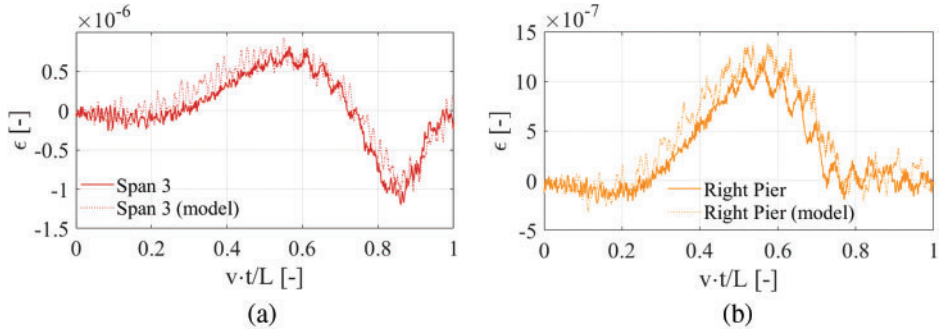

Figure 14. Comparison of the deformation time histories recorded by the sensors and simulated through the calibrated numerical model

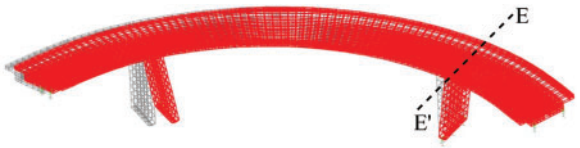

Figure 15. A deformed configuration of the numerical model of the case study bridge, obtained by simulating the evolution of the mountain landslide with the indicated section of the deck triggering the collapse condition

along the direction of the mountainside landslide. As the pier was hinged at both ends, the simulated ground movements did not produce any increase in stress within the deck of the structure. The second set of displacements, applied to the left abutment of the model, was increased up to 50 mm when the collapse condition was reached at section E—E′ of the model's deck. The maximum admissible displacement of the left abutment of the bridge, resulting from the numerical simulation of the landslide phenomenon, was therefore equal to 350 mm.

Considering the growth rate of about 43.8 mm/year characterizing the deformation phenomenon affecting the left abutment of the bridge (determined via InSAR-based monitoring as reported in the previous sections of the paper), and assuming this value to be constant over time, the maximum admissible displacement of the left abutment thus determined via numerical simulations can be reached in approximately 8 years, which is the provisional estimate of the residual life of the structure. It is worth mentioning that several assumptions were made in the computations of the residual life of the case study bridge (e.g., this concern, among others, material properties, modeling strategies, and evolution of the landslide). The influence of each of them in the calculations will be carefully evaluated in future studies, so refinement of the estimate of the residual life of the bridge can be expected.

Conclusions

The paper has proposed a new methodology for the diagnosis and monitoring of bridges and viaducts under the effects of slow deformation phenomena, such as those induced by mountain landslides. InSAR observations play a central role in the approach as they are used both for the remote identification and monitoring of bridges affected by this pathology. Landslides can cause various structural diseases to bridges and viaducts, leading them to collapse in the worst-case scenarios. It follows that the early identification of assets experiencing landslides and their continuous monitoring are tasks of crucial importance to ensure the safety of road networks.

The methodology initially employs SAR screening methods to remotely scan large geographical areas and identify bridges on which satellite-monitored points show irreversible accumulations of deformation in their displacement trends.

Visual inspections are carried out on the detected structures to assess the entity of the deformation phenomena, their interaction with the assets, structural defects, and potential collapse mechanisms. The methodology proposes the adoption of a data-driven or model-based SHM approach for the continuous monitoring of the identified bridges based on the results of visual inspections. Bridges evaluated in a sound health state, characterized by a non-critical interaction with the landslide, can be subjected to continuous InSAR monitoring. In this scenario, thresholds can be defined to trigger alarms caused by anomalies in the trends of the displacements monitored via satellites. Moreover, InSAR observations can be further processed to evaluate potential changes in the structural response of the asset induced by the landslide over time. Bridges experiencing critical structural conditions can instead be monitored in a continuous fashion by combining the analysis of InSAR observations with the outcomes from numerical simulations. Numerical models mimicking the actual structural response of the selected bridges can be defined and used to carry out collapse simulations to estimate the residual life of the structures. The insights obtained from the critical analysis of the numerical outcomes can then be employed to validate/integrate the results obtained via InSAR monitoring and vice versa; such an approach aims at achieving comprehensive structural performance evaluations of the bridges under investigation. With this purpose, field tests can also be carried out on the assets to improve the knowledge of their structural behavior and, therefore, the accuracy of the numerical simulations.

The paper has also presented a case study of a curved road bridge affected by a mountain landslide to provide a practical application of the proposed methodology. The approach leading to the remote identification of the bridge and its slow deformation phenomenon based on InSAR observations has been illustrated. Given the outcomes from the visual inspections carried out on the asset, the model-based SHM approach included in the proposed methodology has been selected to monitor the bridge over time. Collapse simulations have been carried out with a numerical model tuned according to the evidence of several field tests performed on the bridge. Then, the synergic use of InSAR observations and outcomes from numerical simulations permitted the obtainment of a provisional estimate of the residual life of the structure.

Overall, the paper addressed the need for systematic methodologies to account for InSAR data in the diagnosis and monitoring of bridges affected by slow deformation phenomena. Given its large-scale applicability, the proposed methodology can suit the needs of managing authorities dealing with inventories of bridges spread over large geographical areas. As the proposed approach is based on the processing of SAR observations for the remote detection/monitoring of bridges under slow deformation phenomena, the reader can easily understand that the main limitations of the methodology lie in the availability of PSs, with reference to their location and numerosity within a specific area and/or relative to a specific bridge asset, as well as in the temporal length of the SAR measurement series, when available.

Recommendations for future work

The influence of the assumptions made in the residual life calculation of the case study bridge should be systematically evaluated in future studies to refine the estimate found in this work and, no less importantly, to consciously drive structural performance assessments and numerical modeling of future assets affected by slow deformation phenomena. The establishment of monitoring thresholds from InSAR data should be also investigated extensively.

Acknowledegments

This work was financially supported by FABRE—Research Consortium for the evaluation and monitoring of bridges, viaducts, and other structures through funds for basic research on "Multi-level safety analysis and monitoring of existing bridges." The authors gratefully acknowledge funding from the Italian Ministry of University and Research through the PRIN Project "TIMING"—Time evolution laws for IMproving the structural reliability evaluation of existING post-tensioned concrete deck bridges" (protocol no. P20223Y947). The authors would also like to acknowledge the contribution of the e-Geos group for providing the SAR data used in this study. The authors from the University of Perugia also acknowledge funding by the European Union—NextGenerationEU under the Italian Ministry of University and Research (MUR) National Innovation Ecosystem grant ECS00000041—VITALITY. Finally, the authors from the University of Camerino acknowledge the cofounding received from the European Union—FSE, Pon Research, and Innovation 519 2014–2020, for what concerns the research activity carried out within the research project "Synergistic use of innovative sensors and new data analysis procedures for the safety of infrastructures."

Disclaimer

The authors declare no conflict of interest.

Supplemental Materials

Data reported and discussed in this work are available upon request.

References

[1] Zanini MA, Faleschini F, Pellegrino C. Bridge residual service-life prediction through Bayesian visual inspection and data updating. *Struct Infrastruct Eng*. 2017 Jul 3;13(7):906–917. doi:10.1080/15732479.2016.1225311

[2] Nettis A, Saponaro M, Nanna M. RPAS-based framework for simplified seismic risk assessment of Italian RC-bridges. *Buildings*. 2020 Aug 28;10(9):150. doi:10.3390/buildings10090150

[3] Meoni A, García-Macías E, Venanzi I, et al. A procedure for bridge visual inspections prioritisation in the context of preliminary risk assessment with limited information. *Struct Infrastruct Eng*. 2023 May 3;2:1–27. doi:10.1080/15732479.2023.2210547

[4] Casas JR, Cruz PJ. Fiber optic sensors for bridge monitoring. *J Bridge Eng*. 2003 Nov;8(6):362–373. doi:10.1061/(ASCE)1084-0702(2003)8:6(362)

[5] Kim S, Kim T. Machine-learning-based prediction of vortex-induced vibration in long-span bridges using limited information. *Eng Struct*. 2022;266(4):114551. doi:10.1016/j.engstruct.2022.114551

[6] Anastasopoulos D, De Roeck G, Reynders EPB. One-year operational modal analysis of a steel bridge from high-resolution macrostrain monitoring: influence of temperature vs. retrofitting. *Mech Syst Signal Process*. 2021;161(9):107951. doi:10.1016/j.ymssp.2021.107951

[7] Scozzese F, Dall'Asta A. Nonlinear response characterization of post-tensioned RC bridges through Hilbert-Huang transform analysis. *Struct Control Health Monit*. 2024 Feb 23;2024. doi:10.1155/2024/5960162

[8] Milillo P, Giardina G, DeJong MJ, et al. Multi-temporal InSAR structural damage assessment: The London crossrail case study. *Remote Sens*. 2018 Feb 13;10(2):287. doi:10.3390/rs10020287

[9] Zhu M, Wan X, Fei B, et al. Detection of building and infrastructure instabilities by automatic spatiotemporal analysis of satellite SAR interferometry measurements. *Remote Sens*. 2018;10:1816. doi:10.3390/rs10111816

[10] Cavalagli N, Kita A, Falco S, et al. Satellite radar interferometry and in-situ measurements for static monitoring of historical monuments: the case of Gubbio, Italy. *Remote Sens Environ*. 2019;235:111453. doi:10.1016/j.rse.2019.111453

[11] Mele A, Miano A, Di Martire D, et al. Potential of remote sensing data to support the seismic safety assessment of reinforced concrete buildings affected by slow-moving landslides. *Arch Civ Mech Eng*. 2022;22:492. doi:10.1007/s43452-022-00407-7

[12] Giordano PF, Turksezer ZI, Previtali M, et al. Damage detection on a historic iron bridge using satellite DInSAR data. *Struct Heal Monit*. 2022;21:2291–2311. doi:10.1177/14759217211054350

[13] Qin X, Ding X, Liao M, et al. A bridge-tailored multi-temporal DInSAR approach for remote exploration of deformation characteristics and mechanisms of complexly structured bridges. *ISPRS J Photogramm Remote Sens*. 2019;156:27–50. doi:10.1016/j.isprsjprs.2019.08.003

[14] Schlögl M, Widhalm B, Avian M. Comprehensive time-series analysis of bridge deformation using differential satellite radar interferometry based on Sentinel-1. *ISPRS J Photogramm Remote Sens*. 2021;172:132–146. doi:10.1016/j.isprsjprs.2020.12.001

[15] Farneti E, Cavalagli N, Costantini M, et al. A method for structural monitoring of multispan bridges using satellite InSAR data with uncertainty quantification and its pre-collapse application to the Albiano-Magra Bridge in Italy. *Struct Heal Monit*. 2022;0:1–19. doi:10.1177/14759217221083609

[16] Nettis A, Massimi V, Nutricato R, et al. Satellite-based interferometry for monitoring structural deformations of bridge portfolios. *Autom Constr*. 2023 Mar 1;147(46):104707. doi:10.1016/j.autcon.2022.104707

[17] Tonelli D, Caspani VF, Valentini A, et al. Interpretation of bridge health monitoring data from satellite InSAR technology. *Remote Sens*. 2023;15(21):5242. doi:10.3390/rs15215242

[18] Costantini M, Falco S, Malvarosa F, et al. Persistent scatterer pair interferometry: approach and application to COSMO-SkyMed SAR data. *IEEE J Sel Top Appl Earth Obs Remote Sens*. 2014 Jul;7(7):2869–2879. doi:10.1109/JSTARS.2014.2343915

[19] García-Macías E, Ubertini F. MOVA/MOSS: two integrated software solutions for comprehensive structural health monitoring of structures. *Mech Syst Signal Process*. 2020 Sep 1;143:106830. doi:10.1016/j.ymssp.2020.106830

[20] Au SK. Assembling mode shapes by least squares. *Mech Syst Signal Process*. 2011 Jan 1;25(1):163–179. doi:10.1016/j.ymssp.2010.08.002

[21] Wilson EL, Habibullah A. *SAP2000 User's Manual*. Berkeley, Calif: Computers and Structures, Inc.; 2003.

[22] Pastor M, Binda M, Harčarik T. Modal assurance criterion. *Proc Eng*. 2012 Jan 1;48:543–548. doi:10.1016/j.proeng.2012.09.551

[23] Standard B. Eurocode—Basis of structural design. Eurocode 0. 2002 Jul 27.

[24] Pinto PE, Franchin P. Eurocode 8-Part 3: assessment and retrofitting of buildings. *Proc Eurocode*. 2011 Mar 17;8:10–11.

[25] Farneti E, Meoni A, Natali A, et al. Structural health monitoring of curved roadway bridges through satellite radar interferometry and collapse simulation. *ce/papers*. 2023;6:907–916. doi:10.1002/cepa.2201

[26] Celati S, Castellani M, Cavalagli N, et al. Operational modal analysis as a tool for bridge model updating. Application to an unconventional case study. In: *International Conference on Experimental Vibration Analysis for Civil Engineering Structures*; 2023 Aug 2; Cham: Springer Nature Switzerland, pp. 1–10. doi:10.1007/978-3-031-39109-5_1